

# On the Transits of Solar System Objects in the Forthcoming PLANCK Mission: Data Flagging and Coeval Multi-frequency Observations

Michele Maris <sup>1</sup> and Carlo Burigana <sup>2</sup>  
on behalf of the PLANCK Collaboration

<sup>1</sup> INAF–OATs, Via Tiepolo 11, I-34143, Trieste, Italy, EU  
email: maris@oats.inaf.it

and

<sup>2</sup> INAF–IASF Bologna, Via Gobetti 101, I-40129, Bologna, Italy, EU  
email: burigana@iasfbo.inaf.it

Accepted for the publication to *Earth, Moon, and Planets*  
June 30<sup>th</sup>, 2009

## Abstract

In the context of current and future microwave surveys mainly dedicated to the accurate mapping of Cosmic Microwave Background (CMB), mm and sub-mm emissions from Solar System will represent a potential source of contamination as well as an opportunity for new Solar System studies. In particular, the forthcoming ESA PLANCK mission will be able to observe the point-like thermal emission from planets and some large asteroids as well as the diffused Zodiacal Light Emission (ZLE). After a brief introduction to the field, we focus on the identification of Solar System discrete objects in the PLANCK time ordered data.

**Keywords:** Solar System: Minor Bodies, Solar System: Major Bodies, Solar System: Zodiacal Light, Space Missions: Planck, Cosmic Microwave Background

**PACS:** 95.85.Bh, 95.85.Fm, 96.30.-t, 98.80.-k

## 1 Introduction

The ESA PLANCK satellite<sup>1</sup>, scheduled for launch in May 2009, will produce nearly full sky maps at the frequencies of 30, 44, and 70 GHz (Low Frequency Instrument, LFI; [1]) and at 100, 143, 217, 353, 545 and 857 GHz (High Frequency Instrument, HFI; [2]) with an unprecedented resolution (FWHM from  $\simeq 33'$  to  $\simeq 5'$ ) and sensitivity (in the range of  $\simeq 10 - 40$  mJy, i.e.  $1 - 10 \mu\text{K}$  in

<sup>1</sup><http://astro.estec.esa.nl/Planck/>

terms of antenna temperature, on a FWHM<sup>2</sup> resolution element). In order to exploit the scientific targets of the mission even the contamination from faint foreground sources has to be accounted for. External planets, Main Belt asteroids (MBAs), and diffuse interplanetary dust will be observed by PLANCK and will represent a relevant source of contamination but, at the same time, a good opportunity for optical and photometric calibration (in the case of planets) and an interesting subject of scientific analysis<sup>2</sup>.

The possibility to observe Solar System sources with PLANCK has been assessed in several works. [4] showed that it will be possible to use the transits of external planets to reconstruct the PLANCK main beam shapes and to measure the Spectral Energy Distribution of the planets. The expected photometric accuracy is better than 1%, being ultimately limited by the accuracy of the instrumental calibration with the cosmological dipole (at least at  $\nu \leq 353$  GHz). [5] pointed out that PLANCK will be able to observe up to  $3 \times 10^2$  MBAs with a  $S/N > 1$  and several tens of them with significantly better  $S/N$  ratios. Starting from the COBE model for the Zodiacal Light Emission (ZLE) [6, 7, 8] presented a study about the possibility of PLANCK to identify and separate the ZLE exploiting the seasonal differences in the ZLE signal associated with the motion of PLANCK within the Solar System. Moreover, [9, 10] discussed the possibility that the thermal emission of trans-Neptunian objects (TNOs) and of comets in the Oort cloud could induce collective distortions in cosmic microwave maps. At last, [11] analyzed in a general way the problem of how to identify possible microwave emissions correlated to the ecliptical plane in the context of the large scale anomalies reported in the WMAP maps.

In this work we address how to plan observations of Solar System objects with ground facilities or space satellites at times almost coeval with the transits of these sources on PLANCK receivers, in the view of multifrequency studies of these objects.

## 2 Observing the Solar System with the PLANCK satellite

PLANCK is a one-axis stabilized satellite orbiting around the L2 Earth-Sun libration point [12]. It is equipped with a 1.5 m effective aperture aplanatic Gregorian telescope the optical axis of which points in a direction separated by an angle  $\beta = 85^\circ$  from the spin axis [12]. During nominal operations the satellite will spin at a rate of 1 r.p.m. allowing the optical axis of the telescope to scan a circle on the sky with a semiaperture of  $85^\circ$  once a minute. To survey the whole sky the spin axis orientation will be kept constant for about 60 minutes, after

---

<sup>2</sup>For a presentation on these topics see e.g. the talk held at the Workshop *Future Ground based Solar System Research: Synergies with Space Probes and Space Telescope*, held at Portoferraio, Isola d'Elba, Livorno (Italy), September 8–12, 2008, with the original title *Diffuse and Point Like Solar System Emissions in the Forthcoming PLANCK Mission* (<http://www.arcetri.astro.it/~elba2008>; for an account on the conference see also [3]).

which it is drifted about  $2.5 \text{ arcmin}^3$ . Different ways of drifting the spacecraft spin axis define different scanning strategies [12, 13, 14]. The spin axis shall never depart more than a few degrees from the instantaneous antisolar direction. In the nominal scanning strategy the spin axis is kept on the ecliptic plane, while in the baseline scanning strategy currently foreseen for PLANCK it will describe a slow precession about the antisolar direction with a semiaperture of  $7.5^\circ$  and a period of six months in order to have complete sky coverage with the whole set of receivers [13]. The two cryogenic instruments hosted in the telescope focal plane, LFI [1] and HFI [2], form an array of feed-horns covering a field-of-view (f.o.v.) of  $\simeq 7^\circ$ . Each feed-horn points to a slightly different direction in the sky with respect to the center of the f.o.v. defined by the telescope optical axis. In most cases the feed-horns of a given frequency are arranged to be aligned along the same direction, parallel to the scan circle defined by the telescope optical axis, as projected on the telescope f.o.v..

The signals collected by each of the feed-horns are detected independently by the satellite on-board electronics. The instrument output is thus a set of data-streams (time ordered data, TODs) representing the variation of the antenna temperature (or of an equivalent quantity) detected as the telescope scans the sky. When coupled with accurate information about the instantaneous pointing direction of each feed-horn, after proper calibration and data-processing, the TODs are combined to produce multi-frequency maps of the sky (see e.g. [15, 16] and references therein).

PLANCK will return to almost the same heliocentric coordinates every 12 months but it will complete each sky survey in about 7–8 months. Because of the value of  $\beta$  and the locations of the feed-horns, PLANCK will observe Solar System objects in a narrow range of elongations ( $\sim 95^\circ \pm 4^\circ$ ) so that the objects of the inner Solar System can not be observed. Sources will be observed by PLANCK only when they will cross the PLANCK f.o.v. during its scanning of the sky (note that PLANCK is not a space observatory). There is also a certain intrinsic small uncertainty in predicting in advance the exact pointing direction of each feed-horn as a function of time: a precise time / pointing correlation will be established only a posteriori on ground. Also, the same object will be not observed at the same time by all the feed-horns.

As an example, we consider the observations of MBAs and planets in the case of a mission with launch on April 12<sup>th</sup>, 2009 (JD = 2454935.5)<sup>4</sup>. In this case the first survey will start about 45 days after the launch (May 12<sup>th</sup>, 2009), and it will end 258 days after the launch (December 27<sup>th</sup>, 2009). This marks the begin of the second survey which will end 471 days after launch (July 28<sup>th</sup>, 2010). Since a few details of the current baseline scanning strategy are still being defined, we report here results based on the nominal scanning strategy. Our results are only weakly dependent on the exact scanning strategy. The simulation has been performed by using the JPL *Horizons* Ephemeris web server<sup>5</sup>. Other

---

<sup>3</sup>Recently, a constant spacing (of 2 arcmin), instead of a constant time step, has been agreed.

<sup>4</sup>This was the planned launch date at the date of the Workshop.

<sup>5</sup><http://ssd.jpl.nasa.gov/horizons.cgi>, with code for 500@ – 489 PLANCK.

missions have developed their own tools (see e.g. [17]) for this type of task. The PLANCK/LFI consortium adopted Horizons as the reference tool for such kind of calculations for three reasons. Firstly, Horizons will be the official service by which the detailed PLANCK orbit will be disseminated outside the PLANCK collaboration. Horizons allows the recovery of the PLANCK orbit for the nominal launch date and to compute the apparent position of any Solar System object as seen from PLANCK. For a given object it is quite simple to estimate the observability within the PLANCK f.o.v. by looking at its solar elongation. Second, our task is not only to identify which objects enter the PLANCK f.o.v. at a given time, but also to predict precisely their positions with respect to each PLANCK beam rotating about the spin axis, which can be easily accomplished by using the apparent ecliptical coordinates provided by Horizons. Third, the number of objects to be tracked is limited to the five external planets and a relatively small set of MBAs potentially able to affect PLANCK data significantly.

The antenna temperature of an asteroid of radius  $R$  observed at a distance  $\Delta$  from PLANCK is computed by using the simple equation [5]

$$T_{\text{ant},\nu} \simeq 4 \ln 2 e^{-4 \ln 2 \hat{d}^2 / b_\nu^2} \frac{K_\nu}{[b_\nu/\text{radians}]^2} \left[ \frac{R}{\Delta} \right]^2 T_{\text{b},\nu}; \quad (1)$$

here  $b_\nu$  is the FWHM of the feed-horn at the considered frequency channel,  $K_\nu \leq 1$  the photometric efficiency of the considered feed-horn,  $T_{\text{b},\nu}$  the mean surface brightness temperature of the body, and  $\hat{d}$  is the angular distance of the object from the feed-horn center.

Since  $T_{\text{ant},\nu}$  is proportional to  $[R/\Delta]^2$ , only a small fraction of all of the MBAs are relevant for PLANCK. [5] was dedicated to the study of those objects observable in at least some PLANCK feed-horn with a  $S/N > 1$ , equivalent to asteroids with  $T_{\text{ant},\nu}$  of several  $\mu\text{K}$ , corresponding to  $R/\Delta > 2 \times 10^{-7}$  and leading to about 300 MBAs observable asteroids. However, for the accurate exploitation of PLANCK data it is important to take track of all the foreground sources which could induce a contamination in one or more of the PLANCK feed-horns. To have a significant contamination, a point source should have an antenna temperature of at least  $1\mu\text{K}$ . From eq (1) this threshold is equivalent to take MBAs having  $R/\Delta > 5 \times 10^{-8}$  at the epoch of observation. Since  $\Delta$  at the epoch of observation depends on details such as the scanning strategy and the exact satellite orbit, we defined our sample of large MBAs by taking all the objects having  $R/\sqrt{R_{\text{per}}^2 - (1.01 \text{ A.U.})^2} > 5 \times 10^{-8}$ , where  $R_{\text{per}}$  is the asteroid mean perihelion distance.

In order to illustrate the observability function of asteroids in the PLANCK f.o.v., we use a reference frame comoving with the spacecraft spin axis having for  $X$ -axis the spin axis, the  $Y$ -axis aligned with the spin axis drift direction, and the  $Z$ -axis directed toward the North Ecliptic Pole (NEP).

The polar plot in Fig. 1 represents the position of the 1221 MBAs selected on the basis of the above criterion plus all the external planets at 00:00 UT of day 407 after the launch. We define the plotting convention used to draw the figure as the “PLANCK-eye” projection. The objects are drawn in the  $Y, Z$

plane of the spin axis reference frame defined above with  $\varphi$  being the azimuthal direction of an object when projected in the same plane. The normalized radial coordinate is defined as:

$$t = \frac{\theta - \beta}{b_{\text{deg}}} \quad (2)$$

$$\mathcal{N} = \left( 1 - e^{-\left(\frac{180^\circ - \beta}{b_{\text{deg}}}\right)^\varpi} \right)^{1/\zeta} - \left( 1 - e^{-\left(\frac{\beta}{b_{\text{deg}}}\right)^\varpi} \right)^{1/\zeta} \quad (3)$$

$$\rho(t) = \frac{1}{\mathcal{N}} \left[ 1 + \text{sign}[t](1 - e^{-|t|^\varpi})^{1/\zeta} \right], \quad (4)$$

$$\text{sign}[t] = \begin{cases} +1, & t \geq 0 \\ -1, & t < 0, \end{cases} \quad (5)$$

where  $0 \leq \rho(\theta) \leq 1$ ,  $\beta = 85^\circ$  is the angle between the telescope line of sight and the spin axis;  $b_{\text{deg}}$  is a FWHM representative of the instrument;  $\varpi$  and  $\zeta$  are scaling parameters. Here we take  $b_{\text{deg}} = 0.5^\circ$ ,  $\varpi = \zeta = 0.25$ . The scale of the radial coordinate is normalized to have,  $\rho = 0$  for  $\theta = 0^\circ$ ,  $\rho = 1$  for  $\theta = 180^\circ$  and  $\rho = 0.5$  for  $\theta = 85^\circ$ . Those scaling parameters are chosen to smoothly “enlarge” the sky region with  $82^\circ \leq \theta \leq 88^\circ$  which on a linear scale would be too narrow to be seen. Outside that region the relation between  $\rho$  and  $\theta$  is compressed and not linear. In the plot an example of instantaneous location of the rotating f.o.v. is represented by the gray rectangle, the circles represents the region scanned by the f.o.v.. Dots represents the position of the asteroids which are outside of the path of the feed-horns, and that consequently are not observed in the given pointing period. Diamonds the position of observable asteroids. All the objects resides close to the ecliptic, corresponding to  $Y \approx 0$ . Due to the polar singularity, there is an apparent divergence of objects near  $\rho = 1$  (i.e.  $\theta = 180^\circ$ ). The spin axis drifts toward the  $Y > 0$  direction and defines a leading and a trailing edge of the circle. At the trailing edge Mars already left the scan circle after having transited in it, while Saturn is going to transit. At the leading edge Neptune is transiting while Jupiter and Uranus are going to transit and are overlapped due to the plot scale. For completeness the apparent positions of L2, Sun, Moon and Earth, all behind the spacecraft, are also marked.

The relative motion of the objects with respect to the telescope axis scan circle is dominated by the drift directed toward the  $Y > 0$  (or leading) edge of the scan circle. All the objects enter the leading edge of the scan circle and leaves it from the trailing edge more or less moving parallel to the ecliptic. An object crossing the scan circle from the right to the left of the plot will produce a peak in the data-stream with a one minute period and a varying amplitude as it moves through the f.o.v.. Each feed-horn will track a well-defined scan circle, relatively close to that identified by the telescope axis. Each object will cross the scan circles corresponding to the various feed-horns in a sequence and at different times.

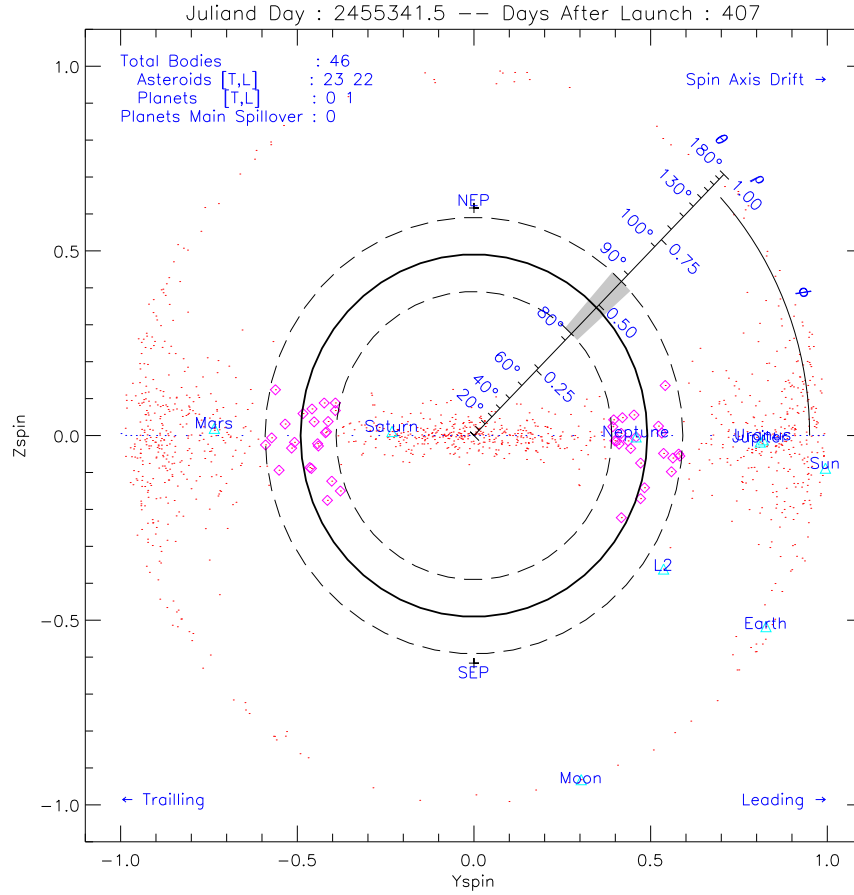


Figure 1: PLANCK-eye representation of a PLANCK scan circle (concentric rings) an instantaneous PLANCK f.o.v. (gray region) together with the positions of a selected subset of asteroids and planets. The tilted graduated scale in correspondence of the f.o.v. gives the relation between the normalized radial coordinate  $\rho$  and the angular distance from the spin axis  $\theta$  according to Eq.s (2–5). The spin axis points outside the plot at (0,0) and it drifts toward the positive  $Y$  direction defining the leading and the trailing directions. The position of the ecliptic poles (North, NEP and South, SEP) are also shown. Red dots represents asteroids outside the f.o.v. while those transiting the f.o.v. are marked with a magenta  $\diamond$ .

Table 1: Statistics for the transits of the Solar System objects of our sample in the PLANCK f.o.v. over a 15 months (two surveys) period. For each quantity,  $x$ , the table gives its central value over the selected set of objects and its half-range between the members of the set in the form  $\bar{x} \pm \delta x$ .

Total number of Tracked Objects <sup>a</sup> :	1226
Average Number of Tracked Objects in the f.o.v. *:	$47 \pm 20$ <sup>b</sup>
Fraction of Detectable Tracked Objects :	31%
Fraction of Tracked Objects Crossing the f.o.v. once:	17%
Fraction of Tracked Objects Crossing the f.o.v. twice:	83%
Delay between subsequent transits at leading and at trailing sides:	$164 \pm 6$ days
Typical f.o.v. crossing time:	8–9 days
Apparent f.o.v. crossing speed:	2 arcmin/hours

<sup>a</sup> Including planets from Mars to Neptune.  
<sup>\*</sup> Per pointing period.  
<sup>b</sup> The variation refers to difference about minimum and maximum number.  
<sup>c</sup> Fraction with respect to the total number of tracked objects.

Tab. 1 reports a set of relevant statistics for the transits of the Solar System objects of our sample in the PLANCK f.o.v.. Quantities are presented in the form  $\bar{x} \pm \delta x$  where  $\bar{x}$  is the central value among the subset of bodies (which is very near the corresponding average) and  $\delta x$  is the half-range within the sample. This should not be interpreted as an error or uncertainty in the prediction. The table considers a 15 months period i.e. two surveys. The typical number of objects which may enter the f.o.v. for each pointing period is  $47 \pm 20$  with an obvious equipartition between the leading and the trailing side of each scan circle. Among the objects of our sample, about 31% are potentially detectable in at least one frequency channel. This information combined with the number of objects in the f.o.v., would lead to an expected rate of detections of about 14 per day. However, it has to be considered that most of the detections occur at the highest HFI frequencies whose corresponding feed horns are concentrated in a narrow band near the f.o.v.. This band is crossed by the objects in about one day. When this is taken in account the expected number of detectable objects per day reduces to  $1.6 \pm 0.6$ . Objects may enter the f.o.v. once or twice during the mission. About 17% will enter the f.o.v. once and 83% will enter it twice. Tracked objects are observed twice if they cross the PLANCK f.o.v. both at the leading and the trailing edge of the scan circle. The typical delay between the crossing of the leading and the trailing edge is  $164 \pm 6$  days. The typical time for the objects to cross the leading or the trailing side of the scan circle is about 8 or 9 days, equivalent to say that they cross the f.o.v. at an equivalent speed of about  $\dot{\vartheta}_{\text{fov}} \approx 2$  arcmin/hour. The fact that  $\dot{\vartheta}_{\text{fov}}$  is smaller than the spacecraft drift rate is due to the relative motion of the objects with respect to PLANCK. Since the feed-horns are aligned along slightly different scan circles, the average time in which objects could be observed in their main beam is  $\tau_{\text{vis}} \approx b_{\nu} / \dot{\vartheta}_{\text{fov}}$ .

Table 2: Epochs of transits for planets and some large asteroids through the PLANCK f.o.v.. L: transit at the leading edge of the scan circle. T: transit at the trailing edge.

Mars	L:2009-Oct-27 ÷ 2009-Nov-8	T:2010-Apr-20 ÷ 2010-May-1
Jupiter	T:2009-Oct-29 ÷ 2009-Nov-6	L:2010-Jun-24 ÷ 2010-Jul-2
Saturn	L:2009-Dec-26 ÷ 2010-Jan-2	T:2010-Jun-10 ÷ 2010-Jun-17
Uranus	T:2009-Dec-4 ÷ 2009-Dec-11	L:2010-Jun-23 ÷ 2010-Jun-30
Neptune	T:2009-Nov-4 ÷ 2009-Nov-12	L:2010-May-21 ÷ 2010-May-28
Ceres	L:2010-Mar-24 ÷ 2010-Apr-1	
Pallas	L:2010-Feb-10 ÷ 2010-Feb-19	T:2010-Jul-15 ÷ 2010-Jul-26
Vesta	T:2009-Nov-22 ÷ 2009-Dec-1	L:2010-May-7 ÷ 2010-May-16

This ranges from 16 – 17 hours for a 30 GHz beam down to 2 – 3 hours for a 857 GHz beam. When combined with the number of feed-horns forming each frequency channel,  $N_{\text{dte}}$ , the total integration time is:

$$\tau_{\text{int},\nu} \approx \frac{b_\nu}{\dot{\vartheta}_{\text{fov}} \tau_{\text{point}}} \frac{b_\nu N_{\text{spin}} N_{\text{dte}}}{\omega_{\text{spin}}} N_{\text{obs}}; \quad (6)$$

here  $N_{\text{obs}}$  is the number of observations,  $N_{\text{spin}} \approx 55$  the number of useful spin rotations during a pointing period of  $\tau_{\text{point}} = 3600$  seconds, and  $\omega_{\text{spin}}$  is the satellite spin-rate. With the PLANCK parameters reported in [5],  $\tau_{\text{int},\nu}$  ranges from 350 sec for the 30 GHz channel down to 15 sec for the 857 GHz frequency channel, with a  $\pm 40\%$  spread because of detailed FWHM of the considered feed-horn, exact beam center angular distance from the spin axis direction, and, obviously, object motion. To a first approximation, useful for practical estimates,

$$\tau_{\text{int},\nu} \approx 10^{3.94 - 0.97 \log_{10}(\nu_{\text{GHz}})} \text{ sec}. \quad (7)$$

As an example of the output of our tool, Tab. 2 gives the epochs for the PLANCK observation of planets and three large asteroids, specifying also if the object transit in the PLANCK receiver scan circle occurs at its leading or trailing edge. Changes in the final orbit <sup>6</sup>, as well as spin axis precession, may displace the observation windows by up to about a week with respect to the table.

### 3 Conclusion

We analyzed the observability of Solar System discrete objects, such as asteroids and planets, by the PLANCK satellite. This is crucial to plan almost coeval observations of these sources and to flag those PLANCK data samples which are severely affected by Solar System objects. The main limitation for coeval

<sup>6</sup>Included the launch delay from Mid April to Mid March.

multifrequency observations comes from the fact that PLANCK will only observe each object more or less in quadrature with the Sun. Since PLANCK will keep its spin axis within some degrees from the antisolar direction, a rough plan for coeval observations can be organized by looking at the elongation of the objects with respect to the Sun. On the other hand, a fine analysis requires to use on-the-shelf ephemerides calculators and the available information about PLANCK focal plane and scanning strategy. Our study shows that the majority of the Solar System objects will be observed at least twice during the nominal mission and allows us to provide statistics of their transits in the PLANCK f.o.v. as well as the corresponding detailed prediction for each object. MBAs will be observed at an average distance from PLANCK of about 2.3 AU so that only asteroids with radii larger than some tens of kilometers will be observed with a sufficiently high S/N ratio. On average at least one or two of such objects will be in the PLANCK f.o.v. each day.

## acknowledgements

This work has been partially supported by the Italian ASI Contract “PLANCK LFI Activity of Phase E2” and by the “Fondi FFO ricerca libera 2009”. We thank Thomas Mueller for constructive discussions. The authors acknowledge the anonymous referee for the accurate reading of the test and the constructive suggestions which aid at improve considerably the text.

## References

- [1] Mandolesi, N., et al., *PLANCK Low Frequency Instrument, A Proposal Submitted to ESA*, (1998)
- [2] Puget, J.-L., et al., *High Frequency Instrument for the PLANCK Mission, A Proposal Submitted to ESA*, (1998)
- [3] Käuff, H.U., Tozzi, G.P., *Report on the Conference Future Ground-based Solar System Research: Synergies with Space Probes and Space Telescopes* The Messenger, 184, 56–57, (2008) (<http://www.eso.org/sci/publications/messenger/archive/no.134-dec08/messenger-no134-56.pdf>)
- [4] Burigana, C., Natoli, P., Vittorio, N., Mandolesi, N., Bersanelli, M., *In-flight main beam reconstruction for PLANCK/LFI*, *Experimental Astronomy*, 12/2, 87–106, (2001)
- [5] Cremonese, G., Marzari, F., Burigana, C., Maris, M., *Asteroid detection at millimetric wavelengths with the PLANCK survey*, *New Astronomy*, 7, 483–494, (2002)
- [6] Kelsall, T., Weiland, J.T., Franz, B.A., et al., *The COBE Diffuse Infrared Background Experiment Search for the Cosmic Infrared Background. II. Model of the Interplanetary Dust Cloud* ApJ, 508, 44–73, (1998)

- [7] Fixsen, D.J., Dwek, E., *The Zodiacal Emission Spectrum as Determined by COBE and Its Implications* Ap. J., 578, 1009–1014, (2002)
- [8] Maris, M., Burigana, C., Fogliani, S., *Zodiacal light emission in the PLANCK mission*, A&A, 452, 685–700, (2006)
- [9] Babich, D., Blake, Cullen H.; Steinhardt, Charles L. *What Can the Cosmic Microwave Background Tell Us about the Outer Solar System?*, Ap. J., 669, 1406–1413, (2007)
- [10] Babich, D., Loeb, A., *Imprint of distortions in the Oort Cloud on the CMB anisotropies*, New Astronomy, 14, 166–179, (2009)
- [11] Diego, J.M., Cruz, M., Gonzalez–Nuevo, J., Maris, M., Ascasibar, Y., Burigana, C. *WMAP anomalous signal in the ecliptic plane*, MNRAS, submitted, arXiv:0901.4344v1 [astro-ph.CO], (2009)
- [12] The PLANCK Collaboration, *PLANCK the scientific program*, European Space Agency publication ESA-SCI(2005)1, The Netherlands, (2005)
- [13] Dupac, X., Tauber, J., *Scanning strategy for mapping the Cosmic Microwave Background anisotropies with PLANCK*, A&A, 430, 363–371, (2005)
- [14] Maris, M., Bersanelli, M., Burigana, C., et al., on behalf of the PLANCK collaboration, *The Flexible PLANCK Scanning Strategy* Mem. S.A.It. Supplement, 9, 460–462, (2006)
- [15] Cappellini, B., Maino, D., Albeti, G., Platania, P., Paladini, R., Mennella, A., Bersanelli, M., *Optimized in-flight absolute calibration for extended CMB surveys*, A&A, 409, 375–385, (2003)
- [16] Kurki-Suonio, H., Keihanen, E., Keskitalo, R., Poutanen, T., Sirvio, A.-S., Maino, D., Burigana, C., *Destriping CMB temperature and polarization maps*, A&A, submitted, arXiv:0904.3623 [astro-ph.IM], (2009)
- [17] Barbieri, C., Bernardi, F., Bertini, I., *Asteroidal background for the Wide Angle Camera of the Rosetta Mission* AAS, DPS Meeting #33, #57.12; Bull. of the AAS, 33, 1145, (2001)